



CHORUS

This is the accepted manuscript made available via CHORUS. The article has been published as:

## Polarizing Oxygen Vacancies in Insulating Metal Oxides under a High Electric Field

Mostafa Youssef, Krystyn J. Van Vliet, and Bilge Yildiz

Phys. Rev. Lett. **119**, 126002 — Published 21 September 2017

DOI: [10.1103/PhysRevLett.119.126002](https://doi.org/10.1103/PhysRevLett.119.126002)

# Polarizing oxygen vacancies in insulating metal oxides under high electric field

Mostafa Youssef,<sup>1#</sup> Krystyn J. Van Vliet,<sup>1,2\*</sup> and Bilge Yildiz<sup>1,3\*</sup>

<sup>1</sup>Department of Materials Science and Engineering

<sup>2</sup>Department of Biological Engineering

<sup>3</sup>Department of Nuclear Science and Engineering, Massachusetts Institute of Technology,

77 Massachusetts Avenue, Cambridge, Massachusetts 02139, USA

#Present Address: Department of Mechanical Engineering, The American University in Cairo, AUC Avenue, P.O. Box 74, New Cairo 11835, Egypt

\*Correspondence to: [krystyn@mit.edu](mailto:krystyn@mit.edu) and [byildiz@mit.edu](mailto:byildiz@mit.edu)

## ABSTRACT

We demonstrate a thermodynamic formulation to quantify defect formation energetics in an insulator under high electric field. As a model system, we analyzed neutral oxygen vacancies (color centers) in alkaline-earth-metal binary oxides using density functional theory, Berry phase calculations, and maximally localized Wannier functions. Work of polarization lowers the field-dependent *electric* Gibbs energy of formation of this defect. This is attributed mainly to the ease of polarizing the two electrons trapped in the vacant site, and secondarily to the defect induced reduction in bond stiffness and softening of phonon modes. The formulation and analysis have implications for understanding the behavior of insulating oxides in electronic, magnetic, catalytic, and electrocaloric devices under high electric field.

Growing interest in understanding effects of large electric fields on the polarization, thermodynamics and kinetics of defects in insulating oxides is driven by emerging technologies including resistive switching memories [1,2], electrocaloric refrigeration [3], field assisted ceramic sintering [4], and controlling nanowire growth [5]. Additionally, giant electric fields on the order of 10 MV/cm arise naturally at oxide hetero-interfaces [6,7]. Point defects, particularly oxygen vacancies, play a prominent role in creating interfacial electric fields [8,9] and dictating the functional properties of these metal oxides [10]. The polarization response and thermodynamics of a defect-free insulating crystal under high electric field is well formulated [11–13]. However, the analogous high field effect on a defective crystal remained challenging to address [1,14,15].

Applying a homogeneous electric field  $\vec{E}$  to an insulating crystal bends its electronic bands linearly, and polarizes the crystal uniformly. Thermodynamically, the former effect augments the differential of the internal energy of the crystal  $dU$  by a charge transfer or electrochemical work  $\phi dq$  [12]. Here,  $\phi$  is the electrostatic potential and  $q$  is the charge transferred. The second effect extends  $dU$  by what is known as the polarization work  $\vec{E} \cdot d(V\vec{P})$ , where  $V$  is the crystal volume and  $\vec{P}$  is its macroscopic polarization [12]. A perfect crystal is not affected by  $\phi dq$  since it is neutral. On the contrary, charged defect equilibria in an insulating defective crystal are affected strongly by  $\phi dq$ . This electrochemical effect has been exploited to control the defect equilibria in  $\text{CeO}_2$  [16] and phase transitions in  $\text{SrCoO}_x$  [17]. In contrast, polarization work is well analyzed for perfect crystals [18,19] and was invoked to predict electric field effect on the phase diagram of defect-free water [20] (ions are the defects of liquid water [21]) and on the phase transitions of defect-free  $\text{HfO}_2$  and  $\text{ZrO}_2$  [22]. However, there is no detailed and quantitative analysis for the impact of polarization work on a realistic insulator that

contains point defects. In particular, we seek a thorough analysis that spans from the global effects of electric field on the abundance of defects, down to the local effects on the single defect site. In this letter, we adopt the neutral oxygen vacancy  $V_O^\times$  in MgO, CaO, SrO, and BaO as a model system to study polarization effects. This class of oxides is important due to their abundance on Earth [23], and their potential use in catalysis [24], electronics [25] and even as ferroelectrics [26]. The study of this neutral defect allows us to focus on polarization effects, as we intentionally preclude any contribution from electrochemical work. This defect, which is also known as the color center, is the canonical intrinsic defect in these oxides [27].

In this Letter, using density functional theory (DFT) and modern theory of polarization [28] we reveal that the abundance of  $V_O^\times$  is enhanced by the work of polarization. We attribute this enhancement to two factors; primarily the ease of polarizing the two electrons trapped in  $V_O^\times$ , and secondarily the softening of some phonon modes and reduction in stiffness of bonds in the defective crystal containing  $V_O^\times$ . These conclusions are supported by analyzing the polarization field of the defect, and the static dielectric permittivities of both the perfect and defective crystals.

For an insulating metal oxide under electric field, the first differential of internal energy is:

$$dU = TdS - PdV + \mu_O dN_O + \sum_k \mu_k dN_k + \mu_e dn_e + \phi dq + \vec{\mathbf{E}} \cdot d(V\vec{\mathbf{P}}), \quad (1)$$

where  $T$ ,  $S$  and  $P$  are the temperature, entropy, and pressure, respectively. The chemical potentials  $\mu_O$ ,  $\mu_k$ , and  $\mu_e$  are those of oxygen, cation  $k$ , and electrons, respectively; and  $N_O$ ,  $N_k$ ,  $n_e$ , are the number of particles of oxygen, cation  $k$ , and electrons, respectively. The summation is taken over all types of cations in the oxide. A partial Legendre transform of  $U$  provides a

convenient expression in terms of natural variables that can be varied experimentally such as  $T$ ,  $P$ ,  $\mu_O, \phi$ , and  $\vec{\mathbf{E}}$  [29]. Moreover, for theoretical convenience in treating charged defects, the transform also includes  $\mu_e$  as a natural variable. We define the resulting thermodynamic potential as the *electric* Gibbs free energy and denote this by  $G_E$ :

$$G_E = U - TS + PV - \mu_O N_O - \mu_e n_e - \phi q - V \vec{\mathbf{E}} \cdot \vec{\mathbf{P}}. \quad (2)$$

Here, we restrict the analysis to  $T = 0$  K, assume no electrostriction (hence  $\Delta V = 0$ ), and consider neutral defects (hence  $\Delta q = 0$ ). In addition, following the arguments in reference [20] we do not consider depolarization fields, and as such  $\vec{\mathbf{E}}$  is the applied external field. Under such assumptions we define the electric Gibbs energy of formation,  $G_E^{form}$ , of the neutral defect  $V_O^\times$  to be:

$$G_E^{form} = (U^{def} - U^{perf} + \mu_O) - V \vec{\mathbf{E}} \cdot (\vec{\mathbf{P}}^{def} - \vec{\mathbf{P}}^{perf}), \quad (3)$$

where the superscripts *def* and *perf* denote the defective and perfect crystals, respectively. The first term is the defect formation energy,  $U^{form}$ . The second term in Eq. (3) is the polarization work of primary interest herein, where we identify  $V(\vec{\mathbf{P}}^{def} - \vec{\mathbf{P}}^{perf})$  as the defect dipole moment,  $\vec{\mathbf{p}}_{V_O^\times}$ . In fact,  $U^{form}$  under constant electric displacement field ( $\vec{\mathbf{D}}$ ), which corresponds to open-circuit boundary conditions [19], has been computed previously for neutral defects in thin film Si [30] and TiO<sub>2</sub> [31] using a sawtooth potential. However, under constant  $\vec{\mathbf{E}}$  which corresponds to closed-circuit boundary conditions [19],  $G_E^{form}$  is the relevant thermodynamic potential, and thus the work of polarization is crucial for accurate description of defect thermodynamics under high  $\vec{\mathbf{E}}$ . (See Supplemental Material (SM) [32] section 1.d for more details.)

We calculated the responses of rock-salt MgO, CaO, SrO, and BaO to external electric fields using DFT and Berry phase approach [33,34] as implemented in the QUANTUM ESPRESSO package [35]. Ultrasoft pseudopotentials [36–38] represented the interaction between core and valence electrons and the revised Perdew, Burke, and Ernzerhof functional for solids (PBEsol) [39] described the exchange correlation.  $\vec{E}$  was applied along the cation-oxygen bonds in [100] direction. By removing the arbitrariness in the polarization quantum, we identified the correct polarization branch for each of the perfect and defective crystals, and thereby quantified the work of polarization in Eq. (3) for formation of  $V_o^\times$ . To analyze the local polarization field surrounding the defect site, we invoke the well-established relationship between Wannier centers and polarization [28,40]. Thus, we computed maximally localized Wannier functions [40] from the original polarized Bloch states using the software WANNIER90 [41]. Further details are included in SM [32].

The field dependence of the relative  $G_E^{form}$  of  $V_o^\times$  in the four oxides is shown in FIG. 1(a).  $\Delta G_E^{form}$  decreases monotonically in all cases, though more pronounced in BaO. In FIG. 1(b) the dependence of  $\Delta U^{form}$  is shown, and indicates a monotonic increase in MgO, CaO, and SrO, but an initial increase followed by a decrease for  $|\vec{E}| > 3$  MV/cm in BaO. This behavior of  $\Delta U^{form}$  is attributable to the static permittivities of the defective and perfect crystals as discussed later. The fact that  $\Delta G_E^{form}$  does not follow the behavior of  $\Delta U^{form}$  shows clearly the importance of the polarization work term in Eq. (3), which favors the formation of the defect with increasing electric field by lowering  $\Delta G_E^{form}$ .

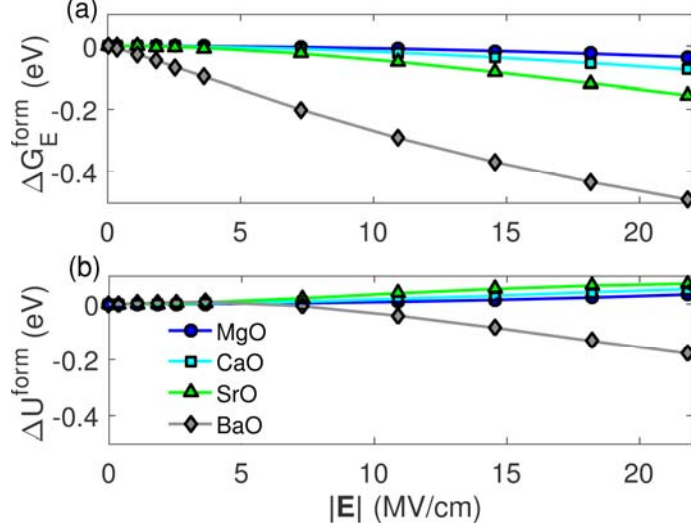


FIG. 1. (a) Relative electric Gibbs free energy of formation and (b) relative formation energy of  $V_O^\times$  as a function of electric field in the studied oxides.

As simple dielectrics, the four oxides exhibit linear  $|\vec{\mathbf{P}}| - |\vec{\mathbf{E}}|$  relationships (Fig. S1 in SM [32]). Nonlinearities arise due to defects. FIG. 2(a) shows the field-dependent dipole moment of  $V_O^\times$  in units of Debye (D). To provide a convenient reference for polarity, we also show the zero-field gas-phase dipole moment of the highly polar water molecule,  $|\vec{\mathbf{p}}_{H_2O}^0|$  of magnitude 1.86 D [42]. At zero-field,  $|\vec{\mathbf{p}}_{V_O^\times}^0| = 0$  as dictated by the symmetry of the rock-salt lattice (see SM section 2 [32]). At finite field, both  $\vec{\mathbf{P}}^{perf}$  and  $\vec{\mathbf{P}}^{def}$  are parallel to  $\vec{\mathbf{E}}$ . Thus a positive value of  $|\vec{\mathbf{p}}_{V_O^\times}|$  implies that  $|\vec{\mathbf{P}}^{def}| > |\vec{\mathbf{P}}^{perf}|$  and this is the case for the four oxides. In MgO,  $|\vec{\mathbf{p}}_{V_O^\times}|$  remains linear with  $|\vec{\mathbf{E}}|$ , and up to the highest field considered here its magnitude remains less than  $|\vec{\mathbf{p}}_{H_2O}^0|$ . Nonlinearity appears in CaO and SrO, in which  $V_O^\times$  can be as polar as gas-phase H<sub>2</sub>O at fields  $> 11.5$  MV/cm and  $> 4.2$  MV/cm, respectively. A more dramatic nonlinearity occurs in BaO where initially  $|\vec{\mathbf{p}}_{V_O^\times}|$  rises to  $7.5|\vec{\mathbf{p}}_{H_2O}^0|$  at a field of 3.6 MV/cm and then reduces

but remains positive up to the highest field considered. The initial sharp increase is due to a reduction in the stiffness of some bonds [43] caused by the creation of the defect. The reduction of  $|\vec{p}_{V_o^\times}|$  at even higher  $|\vec{E}|$  occurs when the bond stiffness around the defect increases relative to that of the perfect crystal under the electric field. We elaborate more on these aspects below.

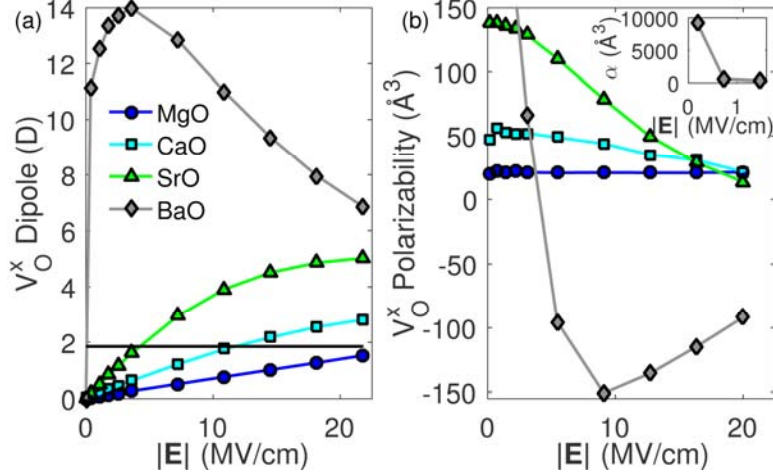


FIG. 2. (a) The field dependence of the dipole moment of  $V_o^\times$ ,  $|\vec{p}_{V_o^\times}|$ . For comparison the zero-field dipole moment of the gas-phase water molecule,  $|\vec{p}_{H_2O}^0|=1.86$  D [42], is indicated by the black horizontal line. (b) Field dependent polarizability of  $V_o^\times$ ,  $\alpha_{V_o^\times}$ . The inset focuses on the low-field polarizability in the case of BaO.

To describe the spatial distribution of the polarization field around the defect site, we define the polarizability tensor of the defect  $\alpha = \partial \vec{p}_{def} / \partial \vec{E}$  which is scalar in this work. We note that our definition does not include dipole-dipole interactions [44,45] since we are concerned here with non-interacting defects. The field-dependent polarizability of  $V_o^\times$  is presented in FIG. 2(b). Magnitudes of  $\alpha$  for  $V_o^\times$  under low (zero)-field are 20, 46, 139, and 9175  $\text{\AA}^3$  in MgO, CaO, SrO, and BaO, respectively, increasing with the size of the host lattice (Section 1.e. in

SM [32]). There have been attempts to compute the low-field polarizability for the color center in alkali metal halides using model Hamiltonians, with reported values ranging between 10 and  $55 \text{ \AA}^3$  [46].

The invariance of  $\alpha$  for  $V_o^\times$  in MgO as a function of  $\vec{E}$  mainly reflects the fact that the field stiffens the bonds in both the perfect and defective crystals at the same pace. In contrast, in CaO, SrO, and BaO,  $\alpha$  is a decreasing function of  $\vec{E}$ , indicating that  $\vec{E}$  stiffens the bonds at a faster pace in the defective crystal. In BaO,  $\alpha$  becomes negative when most of the bonds in the defective crystal become stiffer than their counterpart in the perfect crystal as we explain later with FIG. 4.

A natural question emerges from this discussion: why does work of polarization lower  $G_E^{form}$  of  $V_o^\times$ ? Equivalently, why is the defective crystal more polarized compared to the perfect crystal? We propose two answers. First,  $V_o^\times$  is essentially a vacant site on the oxygen sublattice, containing two trapped electrons. The absence of the confining potential of the nucleus of the removed oxygen atom, together with the vacant space available to the two trapped electrons, facilitates more extensive polarization of these two electrons compared to the polarization of the oxide ion at this position in the perfect crystal. A similar argument is invoked to explain the larger polarizabilities of ions in the gas-phase relative to those in condensed matter [44,47]. Second, the creation of the vacancy softens some phonon modes and reduces the stiffness of the bonds around the vacancy site. These bonds with reduced stiffness are then more polarizable under electric field. We further support these two arguments with the subsequent analysis.

The two electrons trapped in  $V_o^\times$  occupy an in-gap state derived from  $s$ -like orbitals of the surrounding cations (Section 1.f in SM [32]). The zero-field charge densities of these two

electrons in the four oxides considered are depicted schematically in FIG. 3(a-d). An electric field applied along the  $[100]$  or  $+x$  direction deforms the charge density of the two electrons such that it is depleted in  $+x$  and accumulated in  $-x$  as shown in FIG. 3(e-h) under a field of 21.8 MV/cm. This electronic deformation is minimal in the case of MgO, and is very pronounced in BaO.

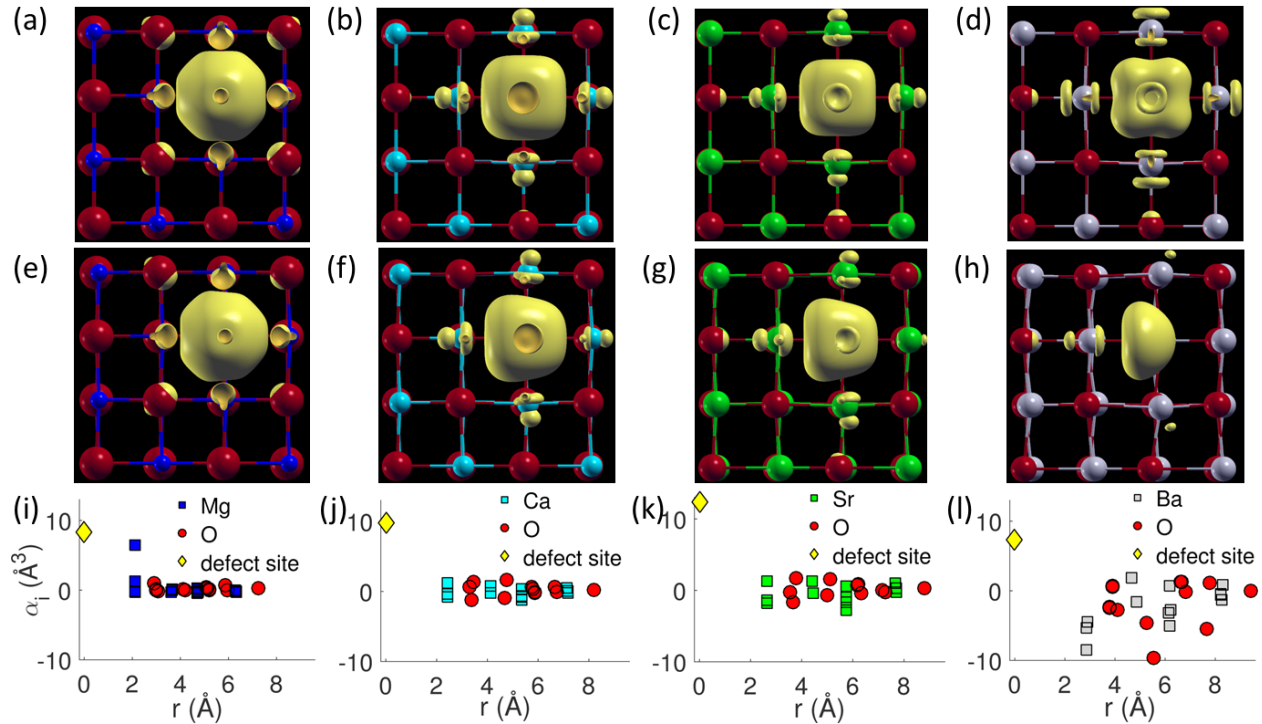


FIG. 3. Visualizations of the charge density of the two electrons trapped in  $V_O^\times$  at zero field in (a) MgO, (b) CaO, (c) SrO, and (d) BaO. Similar visualizations at a field of 21.8 MV/cm in  $+x$  direction are shown for (e) MgO, (f) CaO, (g) SrO, and (h) BaO. Red, blue, cyan, green, and grey spheres represent O, Mg, Ca, Sr, and Ba ions, respectively. The yellow isosurfaces in (a-h) represent the electronic charge density and are taken at 15% of the maximum value in each plot. These visualizations were generated using the software XCRYSDEN [48]. (i-l) show high-field site-decomposed polarizability,  $\alpha_i$ , as a function of distance,  $r$ , from the defect site, in the case of (i) MgO, (j) CaO, (k) SrO, and (l) BaO.  $\alpha_i$ 's were calculated by finite difference between field values of 18.2 and 21.8 MV/cm.

To quantify the contribution of each lattice site to the overall defect polarizability, we compute a site-decomposed polarizability  $\alpha_i$  by invoking the Wannier centers belonging to this lattice site  $i$  such that  $\alpha_{V_o^\times} = \sum_{i \in \text{supercell}} \alpha_i$  (SM section 1c [32]). In FIG. 3(i-l) we present the high-field  $\alpha_i$  for the different lattice sites surrounding the defect. Note that  $\alpha_i$  at the defect site is the difference between the contribution of the two trapped electrons at the defect site in the defective crystal and the contribution of the oxide ion that occupies the very same site in the perfect crystal. It is evident that major contributors to the polarizability of  $V_o^\times$  are the two electrons trapped in the defect site whose high-field  $\alpha_i$  are on the order of  $10 \text{ \AA}^3$ . Even in BaO when the overall high-field  $\alpha$  for  $V_o^\times$  is negative,  $\alpha_i$  remains positive for the two trapped electrons. This supports our first argument that these two trapped electrons are easier to polarize under electric field in comparison to the oxide ion.

The calculated static permittivities of the perfect crystals  $\epsilon^{perf}$  and defective crystals  $\epsilon^{def}$  are shown in FIG. 4. The low(zero)-field  $\epsilon^{perf}$  for the considered oxides are in reasonable agreement with experimental values [49], with the exception of BaO [49,50] (SM section 3 [32]). The figure also shows that the application of  $\vec{E}$  reduces  $\epsilon$  monotonically for all cases. We attribute this decrease to the reduction in the contribution to  $\epsilon$  from the ionic relaxation because the clamped-ion contribution to  $\epsilon$  is field-independent (SM section 3 [32]). The ionic relaxation contribution is inversely proportional to  $\omega_i^2$ , where  $\omega_i$  is the angular frequency of the zone-center phonon mode  $i$  [51]. The field hardens the phonon modes (increases  $\omega_i$ ), and so  $\epsilon$  decreases. FIG. 4 also shows that  $\epsilon^{def}$  is generally greater than  $\epsilon^{perf}$  for all fields with the exception of BaO when  $|\vec{E}| > 3 \text{ MV/cm}$ .  $\epsilon^{def}$  being greater than  $\epsilon^{perf}$  reveals that  $V_o^\times$  softens

some of the phonon modes and reduces the stiffness of bonds in the defective crystal. Since BaO has the largest lattice constant among the studied oxides, introducing  $V_O^\times$  brings BaO to the verge of being ferroelectric as evidenced from the large  $\epsilon^{def}$  at low field shown in FIG. 4(b).

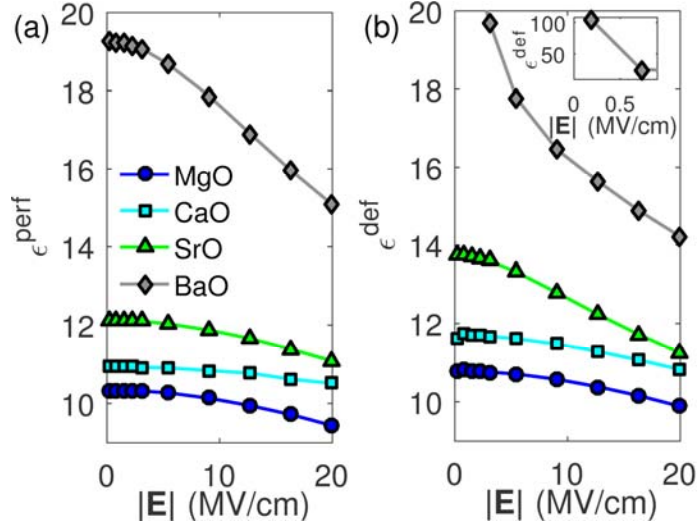


FIG. 4. Field dependent static permittivity of (a) the perfect crystal and (b) the defective crystal containing  $V_O^\times$  for the studied oxides. The inset in (b) focuses on the  $\epsilon^{def}$  of BaO at low fields.

The reduction in bond stiffness introduced by  $V_O^\times$  facilitates bond deformation and stores more associated potential energy under  $\vec{E}$ . Macroscopically, note from Eq. 1 that  $\partial U / \partial \vec{E} = V(\epsilon \epsilon_0 - \epsilon_0) \vec{E}$ , where  $\epsilon_0$  is the vacuum dielectric permittivity. When  $\epsilon^{def} > \epsilon^{perf}$ ,  $\Delta U^{form}$  monotonically increases with  $\vec{E}$ ; this is the case for all of these oxides except BaO at  $|\vec{E}| > 3$  MV/cm, beyond which  $\epsilon^{def}$  becomes less than  $\epsilon^{perf}$ . Note that  $\epsilon^{def} - \epsilon^{perf}$  is essentially the defect polarizability (FIG. 2(b)) scaled by the crystal volume,  $\alpha/V$ . Microscopically and using a harmonic approximation, the energy stored in a bond is  $\frac{1}{2} k \Delta x^2$ , where  $k$  is the bond stiffness and  $\Delta x$  is the bond deformation. Since  $V_O^\times$  reduces the stiffness of some of the bonds,

this increases  $\Delta x$  of these bonds under  $\vec{E}$  and the overall stored potential energy. This explains both macroscopically and microscopically the behavior of  $\Delta U^{form}$  in FIG. 1(b). Since the bonds with reduced stiffness in the defective oxides deform more readily under  $\vec{E}$ , this also means that these bonds are more readily polarized under  $\vec{E}$ . This supports our second argument related to the defective crystal being more polarized than the perfect crystal which eventually contributes to lowering  $G_E^{form}$  of  $V_O^\times$ .

The field itself hardens the phonon modes and increases the bond stiffness in both the perfect and defective crystals.  $V_O^\times$  on the other hand softens the phonon modes and reduces bond stiffness in the defective crystal, and this effect of  $V_O^\times$  prevails against the field effect up to the highest field considered here, except for BaO when  $|\vec{E}| > 3$  MV/cm. Since the defective BaO starts with much softer modes compared to the other oxides, the rate of mode hardening under the field is faster [52] for defective BaO and thus at 3 MV/cm both the perfect and defective BaO have *effectively* similar phonon mode frequencies and bond stiffness (See also SM [32] section 5).

Lastly, we emphasize that  $\Delta G_E^{form}$  is dictated by the relative polarizability of the defective crystal with respect to that of the perfect crystal. This relative polarizability cannot be expressed simply in terms of Born effective charge  $Z^*$  of the cation in the perfect crystal. Although the qualitative order of  $\Delta G_E^{form}$  in FIG. 1(a) matches the order  $Z_{Mg}^* = +2.0 < Z_{Ca}^* = +2.3 < Z_{Sr}^* = +2.4 < Z_{Ba}^* = +2.7$  that we calculated using density functional perturbation theory [53] for the perfect crystals, this does not necessarily hold for all oxides. We support this understanding by calculating the field-dependent  $G_E^{form}$  for  $V_O^\times$  in cubic SrTiO<sub>3</sub> (See

SM section 4 [32] for details and discussion of potential phase transition in SrTiO<sub>3</sub>). In spite of the very large  $Z_{Ti}^* = +6.4$  compared to Ti formal charge of +4 in SrTiO<sub>3</sub> and compared to the cations in the binary oxides, the applied field does not lower  $G_E^{form}$  for  $V_O^\times$  in SrTiO<sub>3</sub> to the same extent as it does in BaO. Perfect crystal SrTiO<sub>3</sub> is highly polarizable as implied by  $Z_{Ti}^*$ , but so is SrTiO<sub>3</sub> containing oxygen vacancies, and the net difference is less than the net difference in polarizability obtained in BaO.

In summary, we investigated the effect of high electric fields on the polarization of neutral oxygen vacancies in alkaline-earth-metal binary oxides. We showed that, beyond the electrochemical effect that is classically null for a neutral defect, the polarization work lowers the *electric* Gibbs energy of defect formation. This was explained by the greater polarizability of the defective crystal compared to the perfect crystal, primarily due to the ease of polarizing the two electrons trapped in the vacant site and due to the reduction in bond stiffness. Accounting for polarization work is necessary for a better understanding of redox based memristive devices. Additionally, our analysis of field-dependent defect polarizability suggests that the assumption of fixed dipoles used in studying electrocaloric refrigerators [54,55] can be relaxed. Future studies can also include implications of defect polarization under electric field on defect diffusion [56].

This work was supported by the MRSEC Program of the National Science Foundation (NSF) under award number DMR – 1419807. This research used resources of the National Energy Research Scientific Computing Center, a DOE Office of Science User Facility supported by the Office of Science of the U.S. Department of Energy under Contract No. DE-AC02-05CH11231. M.Y. thanks Prof. Paolo Giannozzi of University of Udine for helpful comments on Berry phase implementation in QUANTUM ESPRESSO.

- [1] R. Waser, R. Dittmann, G. Staikov, and K. Szot, *Adv. Mater.* **21**, 2632 (2009).
- [2] M. Kubicek, R. Schmitt, F. Messerschmitt, and J. L. M. Rupp, *ACS Nano* **9**, 10737 (2015).
- [3] A. S. Mischenko, Q. Zhang, J. F. Scott, R. W. Whatmore, and N. D. Mathur, *Science* **311**, 1270 (2006).
- [4] H. Majidi and K. van Benthem, *Phys. Rev. Lett.* **114**, 195503 (2015).
- [5] F. Panciera, M. M. Norton, S. B. Alam, S. Hofmann, K. Mølhave, and F. M. Ross, *Nat. Commun.* **7**, 12271 (2016).
- [6] T. Siebert, B. Guchhait, Y. Liu, B. P. Fingerhut, and T. Elsaesser, *J. Phys. Chem. Lett.* 3131 (2016).
- [7] J. Yang, M. Youssef, and B. Yildiz, *Phys. Chem. Chem. Phys.* **19**, 3869 (2017).
- [8] A. F. Santander-Syro, O. Copie, T. Kondo, F. Fortuna, S. Pailhès, R. Weht, X. G. Qiu, F. Bertran, A. Nicolaou, A. Taleb-Ibrahimi, P. Le Fèvre, G. Herranz, M. Bibes, N. Reyren, Y. Apertet, P. Lecoeur, A. Barthélémy, and M. J. Rozenberg, *Nature* **469**, 189 (2011).
- [9] T. C. Rödel, F. Fortuna, S. Sengupta, E. Frantzeskakis, P. L. Fèvre, F. Bertran, B. Mercey, S. Matzen, G. Agnus, T. Maroutian, P. Lecoeur, and A. F. Santander-Syro, *Adv. Mater.* **28**, 1976 (2016).
- [10] H. L. Tuller and S. R. Bishop, *Annu. Rev. Mater. Res.* **41**, 369 (2011).
- [11] J. F. Nye, *Physical Properties of Crystals: Their Representation by Tensors and Matrices* (Clarendon Press, Oxford, 1985).
- [12] R. A. Alberty, *Pure Appl. Chem.* **73**, 1349 (2001).
- [13] N. Bonnet and N. Marzari, *Phys. Rev. Lett.* **113**, 245501 (2014).
- [14] U. Anselmi-Tamburini, G. Spinolo, F. Maglia, I. Tredici, T. B. Holland, and A. K. Mukherjee, in *Sintering*, edited by R. Castro and K. van Benthem (Springer Berlin Heidelberg, 2012), pp. 159–193.
- [15] J. S. Lee, S. Lee, and T. W. Noh, *Appl. Phys. Rev.* **2**, 031303 (2015).
- [16] D. Chen and H. L. Tuller, *Adv. Funct. Mater.* **24**, 7638 (2014).
- [17] Q. Lu and B. Yildiz, *Nano Lett.* **16**, 1186 (2016).
- [18] C. J. Adkins, *Equilibrium Thermodynamics* (Cambridge University Press, 1983).
- [19] M. Stengel, N. A. Spaldin, and D. Vanderbilt, *Nat. Phys.* **5**, 304 (2009).
- [20] J. L. Aragonés, L. G. MacDowell, J. I. Siepmann, and C. Vega, *Phys. Rev. Lett.* **107**, 155702 (2011).
- [21] M. Todorova and J. Neugebauer, *Phys. Rev. Appl.* **1**, 014001 (2014).
- [22] R. Materlik, C. Künneth, and A. Kersch, *J. Appl. Phys.* **117**, 134109 (2015).
- [23] B. B. Karki, R. M. Wentzcovitch, S. de Gironcoli, and S. Baroni, *Science* **286**, 1705 (1999).
- [24] G. Pacchioni and H. Freund, *Chem. Rev.* **113**, 4035 (2013).
- [25] K. J. Hubbard and D. G. Schlom, *J. Mater. Res.* **11**, 2757 (1996).
- [26] E. Bousquet, N. A. Spaldin, and P. Ghosez, *Phys. Rev. Lett.* **104**, 037601 (2010).
- [27] B. Henderson and J. E. Wertz, *Adv. Phys.* **17**, 749 (1968).
- [28] R. Resta and D. Vanderbilt, in *Phys. Ferroelectr.* (Springer Berlin Heidelberg, 2007), pp. 31–68.
- [29] H. B. Callen, *Thermodynamics and an Introduction to Thermostatistics*, Second Edition (John Wiley & Sons, New York, 1985).
- [30] Y. Mao, D. Caliste, and P. Pochet, *J. Appl. Phys.* **114**, 043713 (2013).
- [31] S. Selçuk and A. Selloni, *J. Chem. Phys.* **141**, 084705 (2014).
- [32] See Supplemental Material at [URL Will Be Inserted by Publisher] for Supplemental Methods and Theoretical Approach, the Issue of Zero-Field Vacancy in BaO, Notes on the Calculated Permittivities, Analysis of SrTiO<sub>3</sub>, Discussion of BaO Behavior, and Supplemental References [57- 82].
- [33] P. Umari and A. Pasquarello, *Phys. Rev. Lett.* **89**, 157602 (2002).
- [34] I. Souza, J. Íñiguez, and D. Vanderbilt, *Phys. Rev. Lett.* **89**, 117602 (2002).
- [35] P. Giannozzi, S. Baroni, N. Bonini, M. Calandra, R. Car, C. Cavazzoni, D. Ceresoli, G. L. Chiarotti, M. Cococcioni, I. Dabo, A. Dal Corso, S. de Gironcoli, S. Fabris, G. Fratesi, R. Gebauer, U. Gerstmann, C. Gougoussis, A. Kokalj, M. Lazzeri, L. Martin-Samos, N. Marzari, F. Mauri, R. Mazzarello, S. Paolini, A. Pasquarello, L. Paulatto, C. Sbraccia, S. Scandolo, G. Sclauzero, A. P. Seitsonen, A. Smogunov, P. Umari, and R. M. Wentzcovitch, *J. Phys. Condens. Matter* **21**, 395502 (2009).

- [36] D. Vanderbilt, Phys. Rev. B **41**, 7892 (1990).
- [37] K. F. Garrity, J. W. Bennett, K. M. Rabe, and D. Vanderbilt, Comput. Mater. Sci. **81**, 446 (2014).
- [38] A. Dal Corso, Comput. Mater. Sci. **95**, 337 (2014).
- [39] J. P. Perdew, A. Ruzsinszky, G. I. Csonka, O. A. Vydrov, G. E. Scuseria, L. A. Constantin, X. Zhou, and K. Burke, Phys. Rev. Lett. **100**, 136406 (2008).
- [40] N. Marzari and D. Vanderbilt, Phys. Rev. B **56**, 12847 (1997).
- [41] A. A. Mostofi, J. R. Yates, G. Pizzi, Y.-S. Lee, I. Souza, D. Vanderbilt, and N. Marzari, Comput. Phys. Commun. **185**, 2309 (2014).
- [42] T. R. Dyke and J. S. Muenter, J. Chem. Phys. **59**, 3125 (1973).
- [43] J. J. Gilman, *Electronic Basis of the Strength of Materials* (Cambridge University Press, 2003).
- [44] R. J. Heaton, P. A. Madden, S. J. Clark, and S. Jahn, J. Chem. Phys. **125**, 144104 (2006).
- [45] B. Kozinsky and N. Marzari, Phys. Rev. Lett. **96**, 166801 (2006).
- [46] J. J. O'Dwyer and H. H. Nickle, Phys. Rev. B **2**, 5063 (1970).
- [47] P. W. Fowler and P. A. Madden, J. Phys. Chem. **89**, 2581 (1985).
- [48] A. Kokalj, Comput. Mater. Sci. **28**, 155 (2003).
- [49] K. F. Young and H. P. R. Frederikse, J. Phys. Chem. Ref. Data **2**, 313 (1973).
- [50] R. S. Bever and R. L. Sproull, Phys. Rev. **83**, 801 (1951).
- [51] M. Born and K. Huang, *Dynamical Theory of Crystal Lattices* (The Clarendon Press, Oxford, 1954).
- [52] I. I. Naumov and H. Fu, Phys. Rev. B **72**, 012304 (2005).
- [53] S. Baroni, S. de Gironcoli, A. Dal Corso, and P. Giannozzi, Rev. Mod. Phys. **73**, 515 (2001).
- [54] A. Grünebohm and T. Nishimatsu, Phys. Rev. B **93**, 134101 (2016).
- [55] Y.-B. Ma, A. Grünebohm, K.-C. Meyer, K. Albe, and B.-X. Xu, Phys. Rev. B **94**, 094113 (2016).
- [56] U. Bauer, L. Yao, A. J. Tan, P. Agrawal, S. Emori, H. L. Tuller, S. van Dijken, and G. S. D. Beach, Nat. Mater. **14**, 174 (2015).
- [57] *Standard Solid State Pseudopotentials*, [Http://Materialscloud.org/Sssp/](http://Materialscloud.org/Sssp/) . Accessed 2016-11-21.
- [58] F. Birch, Phys. Rev. **71**, 809 (1947).
- [59] A. Togo, F. Oba, and I. Tanaka, Phys. Rev. B **78**, 134106 (2008).
- [60] H. J. Monkhorst and J. D. Pack, Phys. Rev. B **13**, 5188 (1976).
- [61] S. Speziale, C.-S. Zha, T. S. Duffy, R. J. Hemley, and H. Mao, J. Geophys. Res. Solid Earth **106**, 515 (2001).
- [62] R. C. Whited and W. C. Walker, Phys. Rev. Lett. **22**, 1428 (1969).
- [63] R. Jeanloz and T. J. Ahrens, Geophys. J. Int. **62**, 505 (1980).
- [64] L. Liu and W. A. Bassett, J. Geophys. Res. **78**, 8470 (1973).
- [65] L. Liu and W. A. Bassett, J. Geophys. Res. **77**, 4934 (1972).
- [66] A. S. Rao and R. J. Kearney, Phys. Status Solidi B **95**, 243 (1979).
- [67] J. A. McLeod, R. G. Wilks, N. A. Skorikov, L. D. Finkelstein, M. Abu-Samak, E. Z. Kurmaev, and A. Moewes, Phys. Rev. B **81**, 245123 (2010).
- [68] C. Freysoldt, B. Grabowski, T. Hickel, J. Neugebauer, G. Kresse, A. Janotti, and C. G. Van de Walle, Rev. Mod. Phys. **86**, 253 (2014).
- [69] N. A. Spaldin, J. Solid State Chem. **195**, 2 (2012).
- [70] L. Wang, T. Maxisch, and G. Ceder, Phys. Rev. B **73**, 195107 (2006).
- [71] N. Marzari, A. A. Mostofi, J. R. Yates, I. Souza, and D. Vanderbilt, Rev. Mod. Phys. **84**, 1419 (2012).
- [72] I. Souza, N. Marzari, and D. Vanderbilt, Phys. Rev. B **65**, 035109 (2001).
- [73] K. Momma and F. Izumi, J. Appl. Crystallogr. **44**, 1272 (2011).
- [74] K. Kunc and R. Resta, Phys. Rev. Lett. **51**, 686 (1983).
- [75] Donald A. McQuarrie and John D. Simon, *Physical Chemistry a Molecular Approach* (University Science Books, Sausalito, California, 1997).

- [76] R. P. Lungu, *Thermodynamics of Electric and Magnetic Systems* (INTECH Open Access Publisher, 2012).
- [77] M. Cococcioni and S. de Gironcoli, Phys. Rev. B **71**, 035105 (2005).
- [78] L. Cao, E. Sozontov, and J. Zegenhagen, Phys. Status Solidi A **181**, 387 (2000).
- [79] R. Wahl, D. Vogtenhuber, and G. Kresse, Phys. Rev. B **78**, 104116 (2008).
- [80] K. van Benthem, C. Elsässer, and R. H. French, J. Appl. Phys. **90**, 6156 (2001).
- [81] M. Choi, F. Oba, Y. Kumagai, and I. Tanaka, Adv. Mater. **25**, 86 (2013).
- [82] A. Janotti, J. B. Varley, M. Choi, and C. G. Van de Walle, Phys. Rev. B **90**, 085202 (2014).